

PAPER • OPEN ACCESS

SERS hotspots growth by mild annealing on Au film over nanospheres, a natural lithography approach

To cite this article: A Purwidyantri *et al* 2019 *IOP Conf. Ser.: Earth Environ. Sci.* **277** 012034

View the [article online](#) for updates and enhancements.

SERS hotspots growth by mild annealing on Au film over nanospheres, a natural lithography approach

A Purwidyantri^{1,*}, C-H Hsu², B A Prabowo³, C-M Yang^{2,4,5} and C-S Lai^{2,6,7,**}

¹ Research Unit for Clean Technology, Indonesian Institute of Sciences, Bandung, Indonesia

² Department of Electronic Engineering, Chang Gung University, Taoyuan, Taiwan

³ Research Centre for Electronics and Telecommunications, Indonesian Institute of Sciences, Bandung, Indonesia

⁴ Institute of Electro-Optical Engineering, Chang Gung University, Taoyuan, Taiwan

⁵ Department of General Surgery, Chang Gung Memorial Hospital, Taoyuan, Taiwan

⁶ Department of Nephrology, Chang Gung Memorial Hospital, Taoyuan, Taiwan

⁷ Department of Materials Engineering, Ming-Chi University of Technology, New Taipei City, Taiwan

E-mail: *agnes.purwidyantri@lipi.go.id, **cslai@mail.cgu.edu.tw

Abstract. Surface-enhanced Raman scattering (SERS) detection is a remarkably powerful optical sensing platform employing electromagnetic field amplification in hotspots area produced by nanoparticles. In this study, natural lithography was performed where a 5 nm Au was evaporated on an ITO substrate covered by periodic polystyrene (PS) nanospheres ($d = 100$ nm), called as Au Film over Nanospheres (AuFoN). The substrates went through a rapid thermal annealing (RTA) at 150°C. This temperature was preferred to maintain PS nanospheres from total structural damage while variance in RTA duration at 1, 3 and 5 minutes were applied to investigate the SERS output signal on the treated surfaces. A scanning electron microscopy (SEM) characterization shows the morphological changes of the substrate along with longer RTA duration. Up to 5 minutes of RTA, the periodic trace of PS nanospheres is well-preserved. Based on the atomic force microscope (AFM) screening, the longer RTA process produced higher surface roughness and generated more SERS hotspots. The maximum enhancement factor of SERS signal was obtained by 5 minutes RTA treatment given by the value of 3.16×10^3 . The strong electromagnetic field was shown to be around the spherical line of the nanospheres according to the Finite-Difference Time-Domain method (FDTD) computation.

1. Introduction

SERS phenomenon fundamentally comes from large Raman scattering signals as a result of the presence of nanoparticles (NPs) on a roughened surface [1,2]. There are two major principles contributing to the reinforcement of Raman signals. The first principle, chemical enhancement, refers to the high Raman scattering cross-section of the molecule pertaining to the modified environment in the vicinity of the molecule as well as the chemisorption of the molecules on the metal surface. The second factor is called electromagnetic enhancement and is remarkably attractive due to its ability to yield higher enhancement factor than the first principle, mostly by the Localized Surface Plasmon (LSPR) effects [3,4]. A fantastic enhancement factor of Raman signals is produced by the so-called “hotspots”, nanogaps between NPs generating short-range electromagnetic interaction which allow single molecular detection [5,6]. Due to



its capability of detecting extremely low analyte concentration, SERS has been regarded as a robust technique in diverse areas such as in chemistry, biochemistry, physical and material analysis.

Several attempts have been reported to develop optical sensor in various detection applications from food chemistry to biomedical applications, such as optofluidic [7], surface plasmon resonance sensor [8–10], photonic crystal [11], and colorimetric sensor [12,13]. Nevertheless, the sensitivity performance of these optical sensors was not high enough for very low concentration of target in comparison with SERS technology. Significant works in SERS substrate fabrication denote the synthesise of Au, Ag and Au–Ag alloyed NPs with different size and morphologies, such as particles nanostars [14], Ag/Au core-shell dendrites [15], porous Au nanoparticles (AuNPs) [16], porous Au–Ag alloyed nanocubes [17], and Au/Ag bimetallic nanoparticles [18]. One of the important factors is the uniformity and reproducibility of the SERS substrate. Among many fabrication approaches, the two-dimensional (2D) micro/nanostructured arrays have attracted great attention in regards to excellent uniformity and stability [19,20]. Nanosphere lithography (NSL) generating highly ordered 2D templates using polystyrene-based polymer is typically applied prior to the deposition of metal through solution-dipping or electrochemical deposition techniques [21], physical deposition e.g. by spin-coating [22] or thermal evaporation [23]. Moreover, the NSL process has been noted as “natural lithography”, cutting down the complexity and high cost of conventional photolithography that is mostly conducted in a clean-room. Deposition of metal film over nanospheres (MFO/N) has been a potential trajectory towards SERS hotspots generation due to natural curvature given by the nanospheres and the deposited metallic LSPR effects on it [24–26]. However, trends in research underline the deposition of the considerably thick metal film and only a few studies focus on MFO/N with thin film application (<10 nm thickness).

In this study, surface roughness enhancement and SERS hotspots were obtained through the growth of 5 nm Au nanofilm on the PS nanospheres with a diameter of 100 nm. The gold film over nanospheres (AuFoN) was treated with low-temperature RTA. The RTA process in a considerably low temperature, at 150°C, was aimed to enhance the roughness of the substrate due to partially melted PS and Au agglomeration which led to nanogaps interspacing arrangements for Raman scattering enhancement. The regular order of the small size nanospheres provides a simple nanostructure engineering and natural roughness of the substrate for effective creation of SERS hotspots. The Finite-Difference Time-Domain method (FDTD) simulation was used to study the plasmon coupling behavior of different material interface of AuFoN arrays.

2. Methods

2.1. Gold film over nanospheres (AuFoN) substrate production

The indium tin oxide (ITO) substrate with a geometrical size of 1 cm² was washed and dried with an N₂ flow. After the hydrophilicity of the ITO was achieved, 100 nm diameter PS nanospheres were drop-casted onto the ITO substrate following the methods mentioned elsewhere [27]. In order to reinforce the monolayerity of the nanospheres, the substrates were dried sequentially at room temperature, in an 80°C incubator and on a 100°C hot plate. The PS nanospheres coated surface was then transferred into a thermal evaporation chamber for the deposition of 5 nm Au film obtained by a system setup with the deposition rate of 1 Å/s under 10⁶ mTorr pressure.

2.2. Rapid Thermal Annealing (RTA) treatment on the fabricated AuFoN

Following up the accomplishment of AuFoN structure, the substrates were carried out in an RTA treatment performed in N₂ ambient under the temperature of 150°C for 1, 2, and 5 min. The considerably low temperature used in this work was aimed to maintain the PS nanospheres extreme structural damage while obtaining the increment of surface roughness and gold agglomeration. The SERS substrate fabrication flow and detection mechanism are depicted in Figure 1.

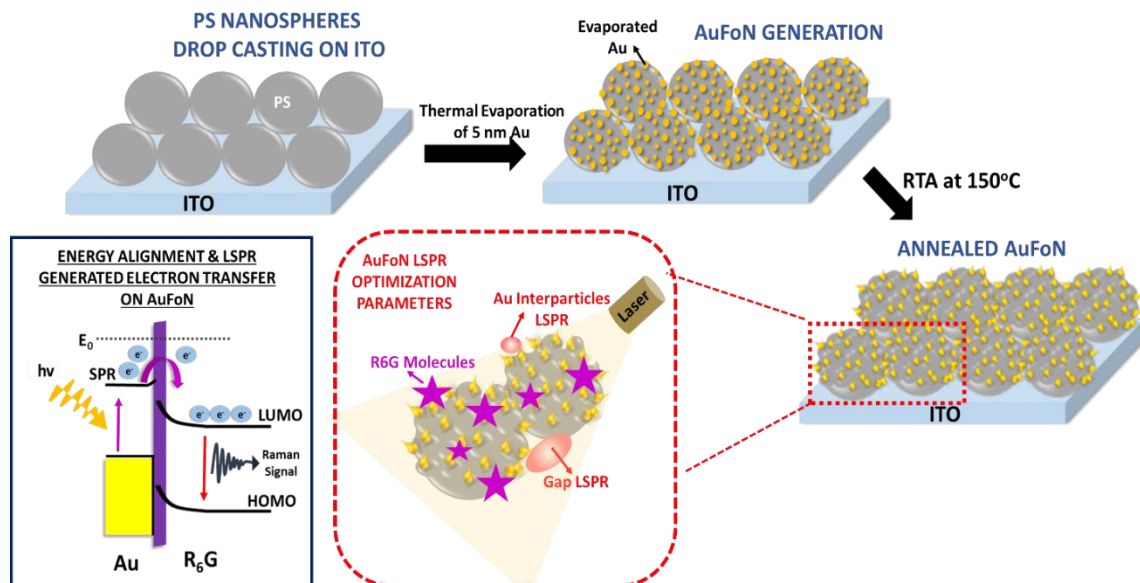


Figure 1. AuFoN fabrication flow, annealing process, R6G SERS detection concept and energy alignment and LSPR generated electron transfer of the proposed method.

2.3. Surface characterization by Scanning Electron Microscope (SEM) and Atomic Force Microscope (AFM)

Every stage of surface modification starting from the covering of PS nanospheres onto ITO substrate was characterized using a HITACHI S-4700 field emission scanning electron microscope (FE-SEM) under an acceleration voltage of 10 kV. The surface roughness of the substrate was analysed using an atomic force microscope (AFM) in tapping mode with a scanning area of $1 \times 1 \mu\text{m}^2$.

2.4. Surface-enhanced Raman Scattering (SERS) characterization of mildly annealed AuFoN and FDTD simulation

SERS measurement applied the RAMaker system from Protrustech.Co, Ltd., with a charge-coupled device (CCD) camera monitoring set and a microscope body. The excitation and collection of light were accomplished by a $100\times$ objective lens (NA 0.5) and an excitation wavelength of 473 nm. A 100 mW excitation laser power was utilized with 2 s exposure time and 3 accumulation numbers. SERS measurement was done to analyze Raman shift response of $1 \mu\text{M}$ Rhodamine 6G (R6G) molecules. The normal Raman spectrum was obtained following the methods mentioned elsewhere [27].

The FDTD simulation was performed using 100 nm of PS nanospheres coated by 2 nm of chromium (Cr) and 5 nm of Au. The optical parameters of Cr and Au were obtained from CRC Materials Science and Engineering Handbook [28], while optical properties for PS nanospheres was taken into account from a previously published result [29]. Subsequently, visible light with a transverse magnetic mode model was utilized for wave coupling.

3. Result and discussion

3.1. Effects of mild RTA on morphological properties of AuFoN

RTA has been noticed as a robust method to be an alternative to other prevalently applied annealing systems, such as that of using tube furnace, which significantly creates a reproducible and uniform plasmonic surface. In this study, we harnessed the low-temperature RTA (150°C) set at 1, 3 and 5 minutes to investigate their impacts on surface roughness enhancement of the AuFoN. The low temperature was fixed with the purpose of avoiding total structural damage of PS nanospheres with the melting point of $283\text{--}398^\circ\text{C}$ [30]. In Figure 2, a gradual transformation of AuFoN morphology was

recorded using an FE-SEM. Figure 2a shows the as-prepared AuFoN monolayer arrays, while Figure 2b, 2c, and 2d are the morphological representations of 1 min, 3 min and 5 min of low-temperature RTA treated AuFoN, respectively. It is clearly depicted that with the prolonged RTA duration, the structural changes of PS nanospheres and Au coalescence were triggered. In this work, a 5 nm thick Au deposited onto the template showed the tendency to form a discontinuous film of isolated Au islands where the growth of lateral grain and changing in such clustered-grain forming structures was limited [31]. The thickness was determined by the deposition adjustment in thermal evaporation setup. In fact, the kinetic process had impacted the deposition of the atom from the vapor phase, such as through thermal facilitation onto the substrate, atomic surface diffusion and dimer formation leading to nucleation and the growing island [3]. Based on the SEM observation, the protrusion on the surface was apparent by 5 min RTA as an outcome of PS structural degradation which concomitantly altered the position of the Au islands residing on top of the nanospheres. It is noteworthy that low-temperature RTA directs the surface profiles of hemispherical particles such as in AuFoN where surface density, mean diameter and surface-to-surface distance are fluctuant with the temperature and exposure time. Generally, the spheres will collapse and substantially decrease in volume as the polymer is heated above 110-120°C [32]. In addition, the monolayerity of the template resists the low heat and thus, maintains the high periodicity after PS structural damage which is critical for SERS hotspots formation.

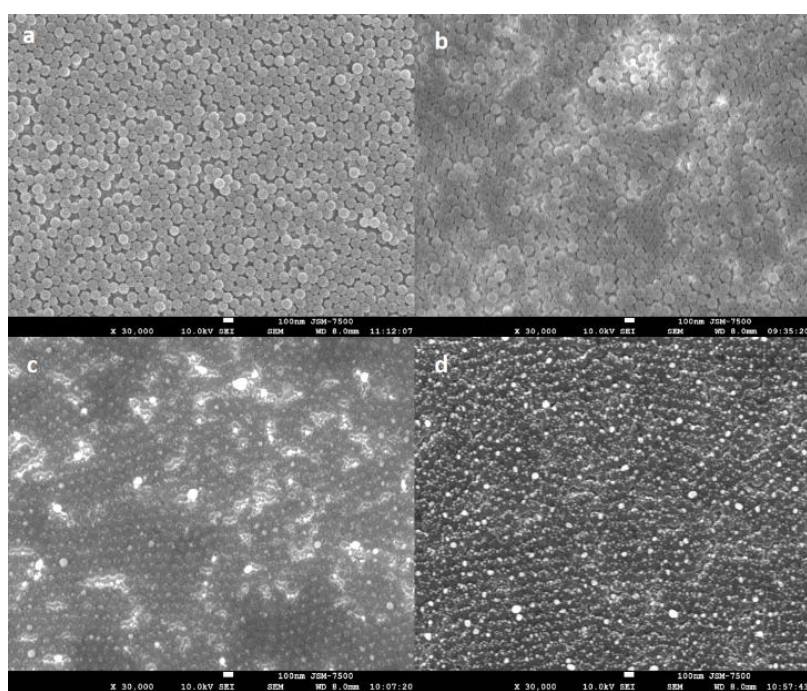


Figure 2. FE-SEM graphs showing the morphological characters of (a) as prepared AuFoN, and AuFoN undergone (b) 1 minute, (c) 3 minute, and (d) 5 minute 150°C RTA treatment.

3.2. Surface roughness enhancement by mild RTA on AuFoN

In order to maintain the periodicity and minimize the PS nanospheres template deformation, RTA was conducted at 150°C with brief exposure. AFM graphs portray the crucial impacts of annealing duration even though set in low-temperature ambience. Figure 3 presents a gradual surface roughness enhancement as the AuFoN undergone RTA, given by ascending Rq values of 8.33, 16.8, and 23.2 nm by 1, 3, and 5 minutes mild RTA, respectively. Several parameters contributed to the enhanced topography of the AuFoN surface; the first one is the curvatures from the partially deformed template with its small diameter (100 nm) and secondly is from Au island coalescence which since the beginning of its deposition process had given tremendous impacts on the roughness.

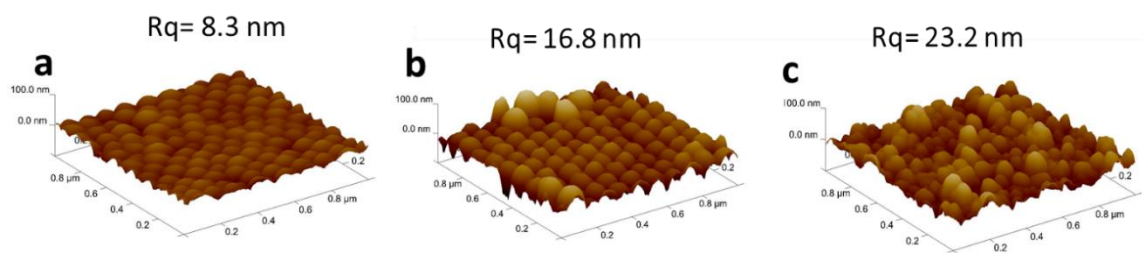


Figure 3. AFM images displaying surface roughness of AuFoN undergone (a) 1 minute, (b) 3 minutes, and (c) 5 minutes mild RTA. Rq value unit is in nanometer (nm).

Au film growth in its initial nucleation stage, since the surface density of the adatoms is extremely low, solely produced primary atomic interaction between the adatoms and the substrate atoms. In a later stage, the interaction occurred between surface deposited adatoms with newly and continuously arriving atoms from the vapor-phase during the deposition. The surface roughness reinforcement in this procedure might arise from a low deposition rate of Au in which the adatoms enabled probing at very high surface area per unit time resulting in prominent nucleation rate at surface defects and high joining rate for diffusing adatoms [33]. Subsequently, it was noticed that mild annealing significantly impacted the height distribution of Au. This is in good accordance with the research of Sui et al [34], who reported that surface roughness could be affected by low-temperature annealing, shown by a height distribution histogram (HDH) of Au droplets annealing in a series of temperature ranging from 50°C-850°C. The contributing factors towards surface roughness (Rq) in this research may favorably create such interstitial nanogaps of 5–20 nm (as roughly counted by the top view AFM dimensional comparison), suitable for the plasmonic “hotspots” formation [35,36].

3.3. SERS properties of mild annealing on AuFoN

SERS measurement was performed to detect 1 μM of Rhodamine 6G (R6G) molecules. Strong Raman bands, exhibiting a typical fingerprint of R6G at around 611, 774, 918, 1197, 1366, 1539, 1573 and 1645 cm^{-1} (inset Figure 4a) [27], differed in position observed in Figure 4a. The SERS spectra output is linearly corresponding to the surface roughness characteristics. It is shown that substantial R6G peaks appeared higher in the AuFoN undergone longer mild annealing. The rougher substrate, as a consequence of longer thermal exposure, created more hotspots which increased the intensity of SERS during R6G analysis. Raman shifts were also captured as the annealing time was prolonged because of the elevation of curvatures affecting the C–H vibrations and C–C stretching modes. The RTA had significantly altered the sub-nanoscale roughness within a single sphere and thus, the impact matched very well with the scattering effect of Raman spectroscopy whilst without RTA, the surface roughness was solely contributed from the spherical curvatures of a single templating particle. Moreover, the shift towards lower wave number with the longer annealing time indicated the enhancement of the local field which was closely linked with red-shifted SPR [37].

The annealing process has been demonstrated to contribute several affecting factors for SERS. One of them is the changing in permittivity after annealing. The annealing procedure tends to force the creation of larger grains leading to boundary region reduction and smaller absorption which finally decrease the imaginary permittivity correlated to the LSPR output [38]. Moreover, to get a profound understanding of SERS detection mechanism in this work, the energy alignment due to surface plasmon resonance (SPR) electron transfer from Au to R6G is illustrated in Figure 1. The LSPR effects were mainly contributed by the formed gap LSPR and Au interparticle LSPR. In order to study the intensive hotspots active sites, a computation on electromagnetic fields distribution on monomer and dimers of thin film Au on top of PS nanospheres was conducted using a Finite-Difference Time-Domain method (FDTD) (Figure 4b). In the monomeric simulation, an intense distribution of electric fields was found to be around the spherical line of the AuFoN, while in the dimeric AuFoNs, the enhancement mostly

occurred on the interstices between two particles as plausible results of the formed gaps and Au interparticle LSPRs.

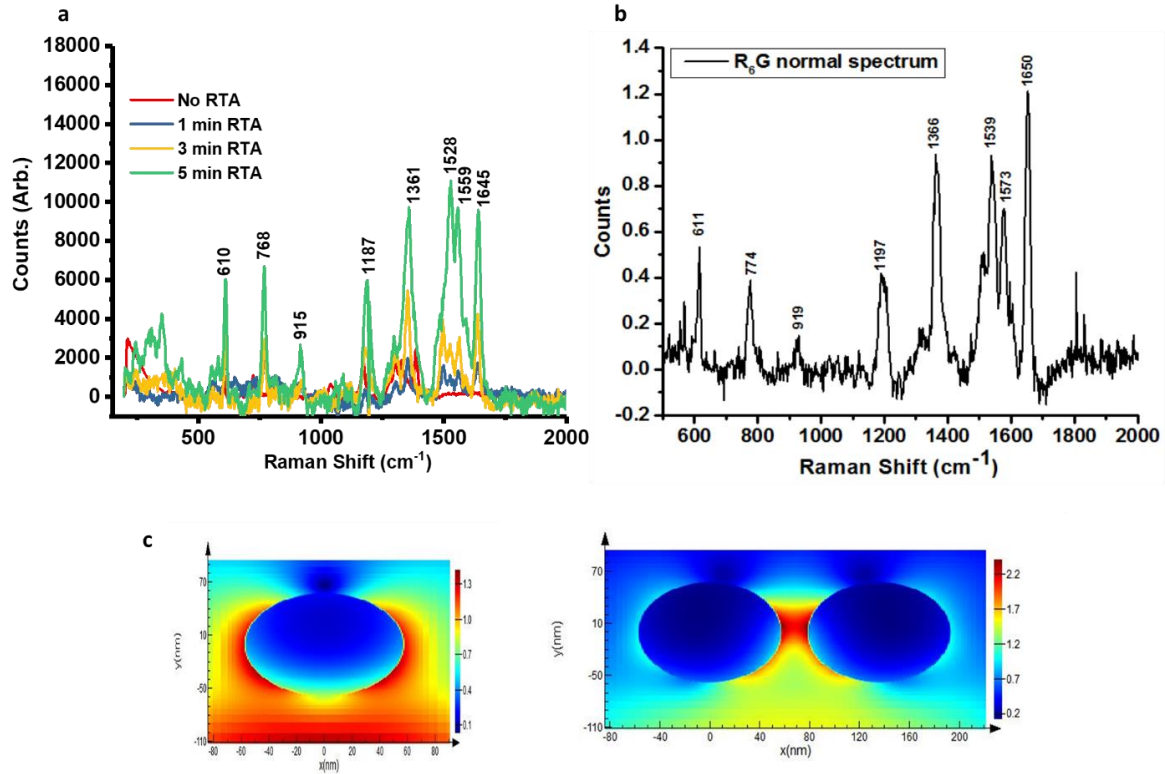


Figure 4. (a) SERS response of 1 μM R6G detection on AuFoN undergone mild annealing with different exposure time, (b) 1 μM R6G normal Raman spectra, (c) Electromagnetic field distribution of the simulated AuFoN using FDTD method (left panel: monomeric AuFoN, right panel: dimeric AuFoN).

3.4. SERS Enhancement Factor (EF_{SERS}) of the annealed AuFoN

The sensitivity of the sensor performance can be quantitatively determined by EF_{SERS} . In this study, we calculated EF by average EF_{SERS} definition using the following equation [27,39].

$$EF_{SERS} = \frac{I_{SERS}/N_{SERS}}{I_{R6G\ norm}/N_{R6G\ norm}}$$

where I_{SERS} and $I_{R6G\ norm}$ are SERS and normal Raman intensities of R6G molecules, while N_{SERS} and $N_{R6G\ norm}$ are the average number of R6G molecules in the scattering volume (V) which contribute to SERS and normal Raman spectrum signals, respectively. The calculation was done using Raman intensity of one of the stable R6G peaks; the 1366 cm⁻¹ peak. The scattering volume based quantification was applied with the approach of the field depth as reported by Liu *et al* [40]. Figure 5 reveals that the exposure time of mild RTA treatment significantly influenced the EF_{SERS} of the AuFoN. The gradual increment of EF_{SERS} is linearly correlated with the profiles of the surface roughness. The highest EF_{SERS} was noticed in 5 minutes mild annealing, given by the value of 3.16×10^3 .

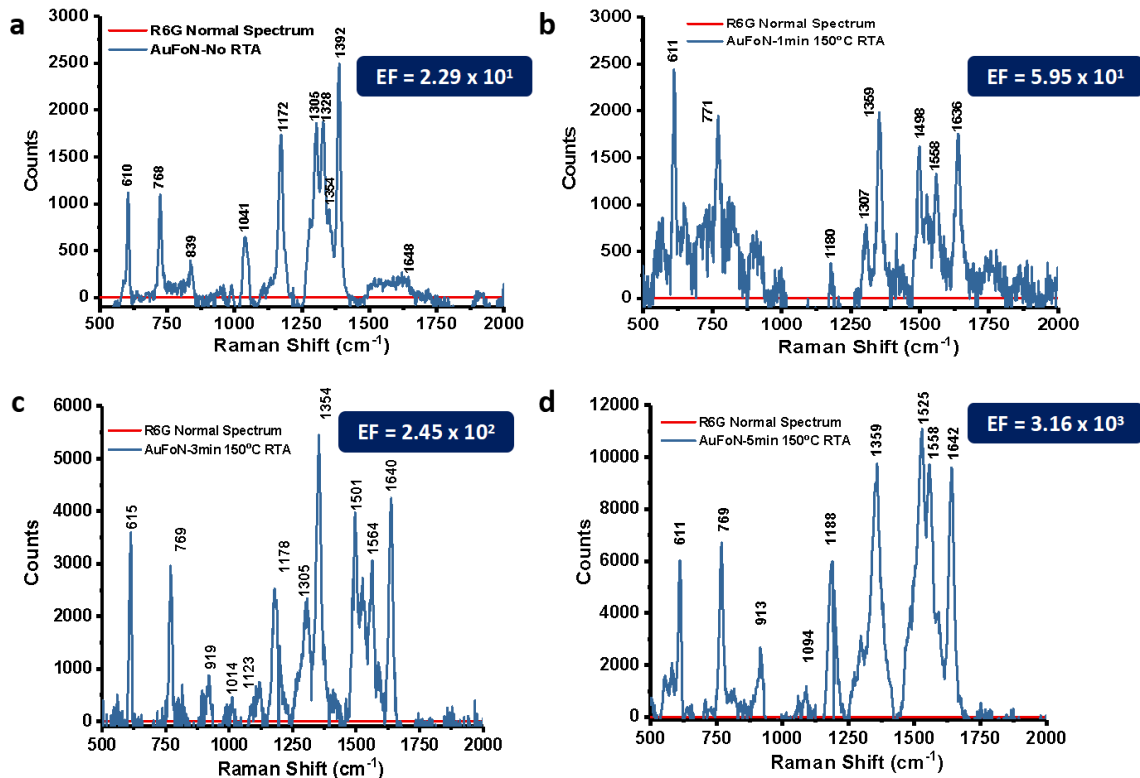


Figure 5. Individual SERS Response of 1 μM R6G detection on AuFoN undergone mild annealing for (a) 0, (b) 1, (c) 3, and (d) 5 minutes and the calculated EF_{SERS} .

4. Conclusion

A mild RTA treatment on AuFoN substrate is reported to exhibit an improvement of plasmonic properties favoring SERS detection as portrayed in the SERS peak intensities of the AuFoN. The process successfully increased the generation of SERS hotspots through several pathways including surface roughness enhancement as a result of partially deformed PS nanospheres template and coalescence of Au islands covering the templates. The FDTD simulation points out strong electric field enhancement along the spherical line of the template where the Au film deposited and between the interstices of two adjacent particles. Mild RTA treatment up to 5 minutes was observed to maintain the periodicity of the template which may help the regularity of the hotspots from the growing nanoparticles. As a future outlook, longer duration of mild annealing and different Au thickness are potential to be used for higher SERS enhancement factor. Overall, the fabricated substrate and the proposed procedure had demonstrated a facile, simple and cost-effective process involving natural lithography as an alternative for high-cost microfabrication applying conventional lithography.

Acknowledgements

The authors thank Chang Gung Memorial Hospital (CGMH) Taiwan, for the financial support under contract no. of CMRPD2G0102; Ministry of Science and Technology (MOST) Taiwan under the contract number of MOST 107-2911-I-182-502 and MOST 107-2218-E-182-006; Kurita Water and Environment Foundation (KWEF) Japan and Asian Institute of Technology (AIT) Thailand for Kurita-AIT Research Grant 2018; and the Indonesian Institute of Sciences.

References

- [1] Lee B S, Lin D Z and Yen T J 2017 *Sci. Rep.* **7** 4604
- [2] Lai C H, Wang G A, Ling T K, Wang T J, Chiu P K, Chau Y F C, Huang C C and Chiang H P 2017 *Sci. Rep.* **7** 5446
- [3] Quan J, Zhang J, Qi X, Li J, Wang N and Zhu Y 2017 *Sci. Rep.* **7** 14771
- [4] Zheng Z, Cong S, Gong W, Xuan J, Li G, Lu W, Geng F and Zhao Z 2017 *Nat. Commun.* **8** 1993
- [5] Radziuk D and Moehwald H 2015 *Phys. Chem. Chem. Phys.* **17** 21072–93
- [6] Köker T, Tang N, Tian C, Zhang W, Wang X, Martel R and Pinaud F 2018 *Nat. Commun.* **9** 607
- [7] Wu S H, Lee K L, Chiou A, Cheng X and Wei P K 2013 *Small* **9** 3532–40
- [8] Prabowo B A, Chang Y F, Lai H C, Alom A, Pal P, Lee Y Y, Chiu N F, Hatanaka K, Su L C and Liu K C 2018 *Sens. Actuators B. Chem.* **254** 742–48
- [9] Prabowo B A, Wang R Y L, Secario M K, Ou P T, Alom A, Liu J J and Liu K C 2017 *Biosens. Bioelectron.* **92** 186–91
- [10] Prabowo B A, Alom A, Secario M K, Masim F C P, Lai H C, Hatanaka K and Liu K C 2016 *Procedia Engineer.* **168** 541–5
- [11] Christiansen M B, Lopacinska J M, Jakobsen M H, Mortensen N A, Dufva M and Kristensen A 2009 *Opt. Express* **17** 2722–30
- [12] Yuan J, Tao Z, Yu Y, Ma X, Xia Y, Wang L and Wang Z 2014 *Food Control* **37** 188–92
- [13] Shinohara S, Tanaka D, Okamoto K and Tamada K 2015 *Phys. Chem. Chem. Phys.* **17** 18606–12
- [14] Niu W, Chua Y A A, Zhang W, Huang H and Lu X 2015 *J. Am. Chem. Soc.* **137** 10460–3
- [15] Yin H J, Chen Z Y, Zhao Y M, Lv M Y, Shi C A, Wu Z L, Zhang X, Liu L, Wang M L and Xu H J 2015 *Sci. Rep.* **5** 14502
- [16] Liu K, Bai Y, Zhang L, Yang Z, Fan Q, Zheng H, Yin Y and Gao C 2016 *Nano Lett.* **16** 3675–81
- [17] Yang Y, Liu J, Fu Z W and Qin D 2014 *J. Am. Chem. Soc.* **136** 8153–6
- [18] Fan M, Lai F J, Chou H L, Lu W T, Hwang B J and Brolo A G 2013 *Chem. Sci.* **4** 509–15
- [19] Pincella F, Song Y, Ochiai T, Isozaki K, Sakamoto K and Miki K 2014 *Chem. Phys. Lett.* **605–606** 115–20
- [20] Zhu S Q, Zhang T, Guo X L and Zhang X Y 2014 *Nanoscale Res. Lett.* **9** 114
- [21] Nguyen V Q, Schaming D, Martin P and Lacroix J C 2015 *ACS Appl. Mater. Interfaces* **7** 21673–81
- [22] Purwidyantri A, Chen C H, Hwang B J, Luo J D, Chiou C C, Tian Y C, Lin C Y, Cheng C H, Lai C S 2016 *Biosens. Bioelectron.* **77** 1086–94
- [23] Purwidyantri A, Kamajaya L, Chen C H, Luo J D, Chiou C C, Tian Y C, Lin C Y, Yang C M and Lai C S 2018 *J. Electrochem. Soc.* **165** H3170–7
- [24] Li J F et al 2013 *Nat. Protoc.* **8** 52–65
- [25] Wang J F, Wu X Z, Xiao R, Dong P T and Wang C G 2014 *PLoS One* **9** e9797
- [26] Farcau C and Astilean S 2010 *J. Phys. Chem. C* **114** 11717–22
- [27] Purwidyantri A, El-Mekki I and Lai C S 2017 *IEEE Trans. Nanotechnol.* **16** 551–9
- [28] Shackelford J F, Han Y H, Kim S and Kwon S H 2015 *CRC Materials Science and Engineering Handbook* 4th Ed. (CRC Press Taylor and Francis Group)
- [29] Sultanova N, Kasarova S and Nikolov I 2009 *Acta Phys. Pol. A* **116** 585
- [30] Zeng W R, Zhou Y J, Huo R, Yao B and Li Y Z *Mater. Sci. Eng.* **22** 162–5
- [31] Herz A, Franz A, Theska F, Hentschel M, Kups T, Wang D and Schaaf P 2016 *AIP Adv.* **6** 035109
- [32] Mehta S, Biederman S and Shivkumar S 1995 *J. Mater. Sci.* **30** 2944–9
- [33] Ruffino F and Grimaldi M 2018 *Coatings* **8** 121.
- [34] Sui M, Li M Y, Kim E S and Lee J 2013 *Nanoscale Res. Lett.* **8** 525
- [35] Bai Y, Gao Z, Chen N, Liu H, Yao J, Ma S and Shi X 2014 *Appl. Surf. Sci.* **315** 1–7
- [36] Arnob M M P, Zhao F, Zeng J, Santos G M, Li M and Shih W C 2014 *Nanoscale* **6** 12470–5
- [37] Tian F, Bonnier F, Casey A, Shanahan A and Byrne H 2014 *Anal. Methods* **6** 9116–23

- [38] Shen P T, Sivan Y, Lin C W, Liu H L, Chang C W and Chu S W 2016 *Opt. Express* **24** 19254-63
- [39] Serrano-Montes A B, de Aberasturi D J, Langer J, Giner-Casares J J, Scarabelli L, Herrero A, and Liz-Marzán L M 2015 *Langmuir* **31** 9205–13
- [40] Liu Y, Xu S, Li H, Jian X and Xu W 2011 *Chem. Commun.* **47** 3784–6